Scientific Research Publishing

Open Journal of Geology, 2025, 15(12), 951-971
https://www.scirp.org/journal/ojg
ISSN Online: 2161-7589
ISSN Print: 2161-7570

Employing Principal Component Analysis and K-Means Clustering to Elucidate the Geological Compositional Process at N'Guérédonké Ultramafic Fe-Ti Deposit

Mohamed Lamine Salifou Sanogo, Ibrahim Wagani

Département de Géologie, Faculté des Sciences et Technique, Université Dan Dicko Dankoulodo, Maradi, Niger
Email: laminesanogo@yahoo.fr

How to cite this paper: Sanogo, M.L.S. and Wagani, I. (2025) Employing Principal Component Analysis and K-Means Clustering to Elucidate the Geological Compositional Process at N'Guérédonké Ultramafic Fe-Ti Deposit. *Open Journal of Geology*, **15**, 951-971.
https://doi.org/10.4236/ojg.2025.1512049

Received: October 30, 2025
Accepted: December 7, 2025
Published: December 10, 2025

Abstract

The N'Guérédonké deposit, Faranah Province (Republic of Guinea), is part of the Leonian-Liberian crystalline shield, consisting of Archean granitoids and greenstone formations with a syn-tectonic ultramafic intrusion. This complex features a dunite core enveloped by wehrlite, pyroxenite, and gabbro, characterized by significant Fe-T mineralization, particularly ilmenite and magnetite in the southern pyroxenite unit, showing the highest TiO_2 grades. The study uses Principal Component Analysis (PCA) on samples to identify correlations among chemical elements. Three main components accounted for 77.01% of the variance (PC1, PC2, PC3), indicating key lithological signatures. K-Means clustering identified four distinct clusters related to lithological characteristics; Cluster 1 as fresh unaltered rocks, Clusters 2 and 4 are associated with Fe-Ti ore whereas Cluster 3 represents alteration patterns with Clusters 2 and 4 identified as priority targets for Fe-Ti ore. NGU has characterized a unique signature of Fe-Ti oxides in ultramafic deposits, such as titaniferous magnetite and chromite spinels, through Fe, Ti, and Cr correlations. Late mobilization of Cu and Zn suggests magmatic fractionation, with a notable negative correlation between SiO_2 and Fe (−0.88) indicating fractional crystallization. The study identifies various clusters based on geochemical analyses, with Cluster 1 reflecting primary lithology and Cluster 3 relating to hydrothermal alterations. Exploration is guided by understanding geochemical complexity in ultramafic deposits.

Keywords

N'Guérédonké, Fe-Ti Deposits, Ultramafic, Magmatic, Fractional Crystallisation, PCA, Clustering, Guinea

1. Introduction

The N'Guérédonké ultramafic (NGU) intrusion (**Figure 1**) is situated within Archean amphibolite gneiss and stretches along a presumed shear zone. The intrusion extends 7 × 0.9 km of NW-SE strike (840 m above sea level), while the entire inferred shear zone has a total strike length of 60 km [1]. Recent mining exploration from BRGM (Bureau de Recherche Géologique et Minière) and AMER (Africa Middle East Resources LTD), a Dubai based company, has notably improved the general knowledge and availability of certain quantities of geological data on the N'Guérédonké ultramafic complex (4 km strike at NW part of the recognized NGUC accounts for the current study). The original nature of magma remains elusive to direct study and observation. However, the lavas available for analysis are believed to reflect the composition of their source rocks, shaped by the physicochemical properties prevailing within thermodynamic envelopes. The composition of magma is primarily determined by two factors: the types of elements present and the general environmental conditions [2]. To better understand ultramafic deposits, it is essential to employ multiple methods beyond petrographic and lithological descriptions. During a mining exploration program or the exploitation of a deposit, large datasets (geochemical, lithological, alteration, structural, etc.) are produced. These tens of thousands of collected data represent an individual observation. Manual analysis of such large dataset is tedious and complex [3].

Statistical analyses, including parameter determination, correlation matrix calculations, and multivariate techniques such as Principal Component Analysis (PCA) and K-means clustering, provide alternative insights into geological organization. Multivariate statistical methods aim to group samples based on common characteristics; these geochemical features they share are also defined by statistical techniques [3]. They reorient these data into a mathematically robust and consistent model so that the best of the variances is observed [3]. The aim of this study was therefore to offer an alternative explanation of the geological construction of the ultramafic body and its mineralization, using chemical rather than petrographic criteria.

2. Geology

The N'Guérédonké deposit is in the Faranah Province of south-central Guinea, approximately 365 km east of Conakry. This deposit is found within the Leonian -Liberian crystalline shield and consists of the Archean Dabola and Kambui granitoids along with greenstone formations. The geological units in the region primarily consist of Early Proterozoic metasomatic and intrusive rocks that have intruded into the granite and gneiss basement from the Late Archean and Early Proterozoic [1]. The N'Guérédonké intrusion is regarded as a syn-tectonic ultramafic intrusion of Ural-Alaskan type. These ultramafic complexes feature zoned intrusive formations with a concentric intrusive pattern comprising a dunite core, which is gradually surrounded by wehrlite, pyroxenite, and gabbro [1]. [1] sees it as a new kind of massive ultramafic intrusion-hosted Fe-Ti deposit, sharing cer-

tain geometric similarities with the initial one but differing from Ural Alaskan due to the absence of orthopyroxenes, chromite pods or layers, and the timing of formation (between 2.94 and 2.1 Ga). These intrusions are typically emplaced at deep levels in the crust and can form lensoid or disk-like bodies (**Figure 1**) of massive or disseminated titanium-vanadium ore [1].

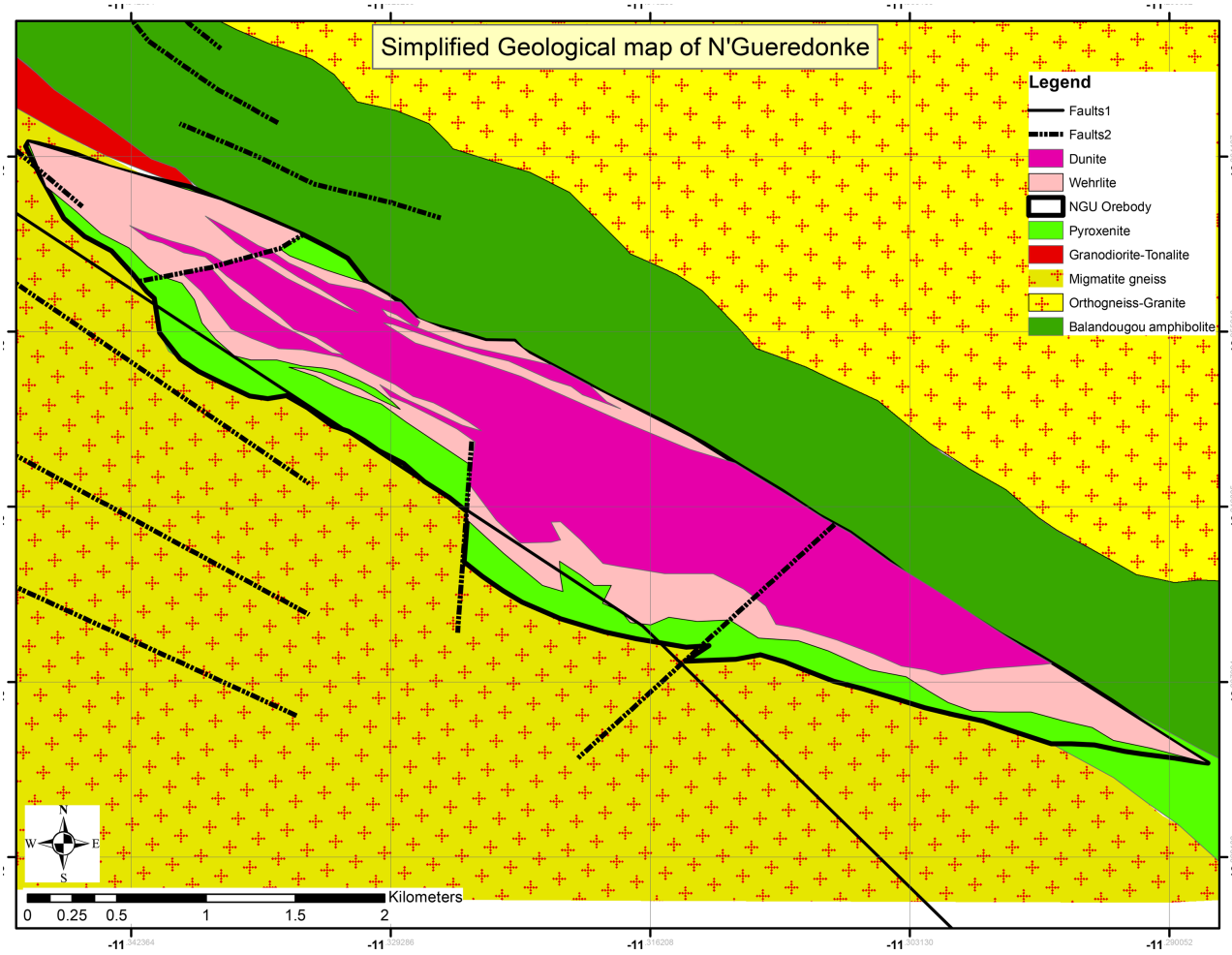

Figure 1. Simplified Geological map of N'Guérédonké (modified after [1] and [4]).

The N'Guérédonké intrusion is hosted within Archean amphibolite gneiss and extends along an inferred shear zone. The concerned portion of the intrusion in this study has 4 km of strike within the overall inferred shear zone of 60 km of strike length in total. The southern section of the intrusion passes outside this studied area (AMER's licence) and goes into its south part of Belzone). At N'Guérédonké a primary magmatic Fe-Ti oxide mineralization is present with titanium as ilmenite ($FeTiO_3$) and titanium dioxide (TiO_2), iron as magnetite (Fe_3O_4) and vanadium as oxide (V_2O_5). The mineralization is dominantly hosted by pyroxenite and magnetite gabbro, both parts of the ultramafic intrusion suite. The most developed Fe-Ti oxide mineralization is currently understood to be in the southern pyroxenite unit. This presents both the highest TiO_2 grade and wid-

est intersections observed from drilling to date.

The pyroxenite when observed in drill core is a medium grained grey-green-black rock with common interstitial magnetite of up to 25%. Composition of the pyroxenite varies depending on the spatial position within the overall intrusion with varying modal percentages of orthopyroxene and clinopyroxene. When wehrlite is observed, this has higher clinopyroxene content with coarser phenocrysts than in the pyroxenites. Whereas mineralogy also includes arsenopyrite, chalcocite and pyrite as observed throughout N'Guérédonké, but this never forms more than 2% of the overall mineralogical composition. The dunite when observed in drill core is a grey-black medium to coarse grained rock with lower interstitial magnetite of 5%.

3. Data Collection and Preparation

Core samples (10,144) from 60 boreholes at different depths ranging from 0 to 600 m drilled by AMER on the N'Guérédonké ultramafic deposit were available and analyzed for major and minor elements and a few trace elements, including Si, Ag, Al, As, Ba, Be, Ca, Cd, Co, Cr, Cu, Fe, Ga, Ka, La, Mg, Mn, Mo, Na, Ni, Pm, Pb, S, Sb, Sc, Sr, Th, Ti, Tl, U, V, W, Zn, Sn, Cl and P and loss on ignition after drying (LOI at 1000˚C) carried out at the ALS laboratory in South Africa. Analytical verification was conducted on 420 (5%) of the samples collected. Correlation matrix was used to select the variables (elements), and multivariate statistical techniques (such as PCA and cluster analysis) were used to group the samples on the basis of common geochemical characteristics predefined by these statistical methods, with a view to providing a different explanation of the geological organization of the ultramafic body, as well as its mineralization, using chemical rather than petrographic criteria. These geochemical and petrographic parameters of the ultramafic body are compared to better understand the internal organization of the mineralized body [5].

Statistical analysis is used to clean up, position, visualize and analyze all these data in space, and view their variance. In this study, we identified statistical parameters, calculated the correlation matrix, and used multivariate statistical methods such as principal component analysis (PCA) and clustering as suggested by [6]. The data analysis and preparation for interpretation were made using ioGAS 7.0 software. The N'Guérédonké Ultramafic body was first explored (core drilling) by six parallel drillhole sections at a 500 m spacing which were drilled up to 250 m below surface and, infill drilling holes with some of them reaching 600 m underneath. The core samples represent the entire recognized ultramafic body and were sampled at 1 m interval. For multivariate study all null analysis were removed and elements below detection limits were replaced by half that value [3] from this study.

4. Results

4.1. Principal Component Analysis (PCA)

Principal Component Analysis (PCA) is an often-powerful statistical method in

these kinds of studies, enabling the dimensionality of the data to be reduced while preserving their main trends [6]. In this study, PCA was applied to the geochemical dataset to identify associations between different elements and very often correctly distinguish lithological signatures [7]. The results, including eigenvalues (**Figure 2**), correlation matrices and biplots, were analyzed and interpreted to extract geochemically relevant conclusions [6].

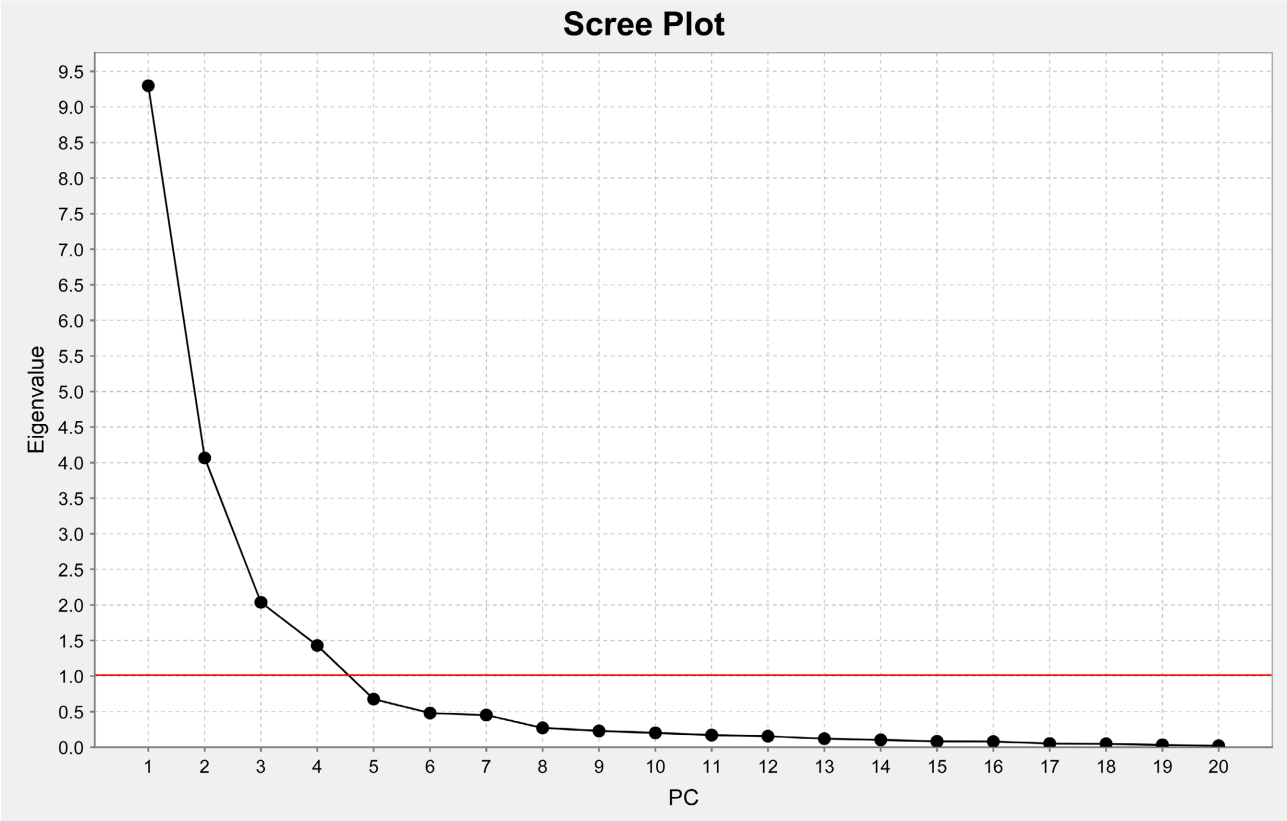

Figure 2. Scree plot showing four (4) PCs with eigenvalues > 1.

The geological environments of ultramafic deposits are very often complex and could involve multiple magmatic, metasomatic, and hydrothermal processes that intersect one another [8] [9]. To distinguish between them and select possible areas of economic interest, the use of multivariate statistical methods such as PCA or K-means clustering [10] is a possible way; though, thousands of data from the NGU deposit could help identify distinctive geochemical signatures, guide mineral exploration and test geological hypotheses in the shear belt. Consequently, PCA is a data analysis technique that uses a data table containing information on both individuals (samples) and quantitative variables (a percentage of the proportion of the chemical element tested in each individual sample) to condense the information. Principal component analysis aims to synthesize the structure of multivariate data by reducing the data to the components of a few, each of these principal components representing a certain percentage of the variability of the data before transformation [6]. PCA produces a summary of information by iden-

tifying similarities between variables. Variables with characteristics that come together to form a group. Links between several variables are used to identify similarities. To achieve this, PCA generates a small set of new variables (the factors: PCs) that capture the characteristics of the entire group of variables. Principal component analysis therefore produces additional variables (PC1 to PC2, PC3, PC4...) with various levels of association with the items [10].

In this study, the use of the correlation matrix plays a key role, as this technique will be used to show the relationships between different pairs of elements. But [6] warned against using standard statistical methods to find correlations and patterns with these kinds of data. Most multivariate methods, including PCA, are designed for Euclidean space rather than "simplex" space and could therefore produce erroneous results [6]. In our case Robust PCA Estimation (RPCA) in line with the recommendations of [11], the classical correlation matrix estimation is replaced by a robust estimation less sensitive to outliers as indicated in [12] with a use of "XY" graphs (bivariate diagram) to visualize and evaluate the results of the PCA study. These diagrams simultaneously visualize the importance (of different variables as vectors (arrows) and the PCA scores calculated for individual samples (dots). The length of an individual arrow is proportional to the variability of the vectors in relation to the two principal components represented, with positively correlated vectors being closer together. The proximity of sample points to specific vectors and their distance from the origin in the diagrams reflect the importance of the influence of these vectors on the sample [12]. For [6] a logarithmic transformation (= logarithms of ratios), a centered log-ratio prior to PCA is necessary, as it converts the compositional data into an unconstrained real space, thus alleviating the closure problem.

The principal component analysis conducted as part of this research used the entire sample set (10,144) of both fresh and weathered core rocks to reveal the main correlations between chemical elements, providing a better understanding of the structure of the data set. As a result, the most powerful indicators highlight the most remarkable patterns (such as a set of interconnected features common to a specific rock type) but also isolate or ignore small occurrences. Hence, the higher the correlation value reaches +1 on the scale, the stronger the correlation between the feature and the PC factor [13] [10].

4.2. Interpretation

PCA reduced the dimensionality of the dataset, with the first three principal components (PCs) explaining 77.01% of the total variance (**Table 1**). The factor PC1 (46.5%) captured the mafic-felsic dichotomy, with positive loadings for Fe, Ni, Cr, and negative loadings for SiO_2 and K (**Figure 3(a)**). While PC2 (20.33%) highlighted carbonate and plagioclase (?) influences (Ca, Na, Mg) (**Figure 3(d)**, **Figure 3(e)**) and PC3 (10.18%) associated with aluminosilicates and clay minerals (Al, Sr). Bivariate plots (e.g., PC1-PC2, PC1-PC3) visualized these relationships, revealing magmatic signatures (PC1 negative: Mg, Ti, Fe), a fluid alteration zones

(PC1 positive: SiO_2, LOI, Ba) and sulfide mineralization potential (PC3 positive: Cu, Zn). An analysis of the eigenvalues and bivariate diagrams shows that the most significant contribution (46.496%) is made by factor PC1, which is composed of a robust relationship between Mg, Ti, Fe, Mn, Zn, V, Ni, Co, Cu, and Sc in a positive series. It could be aligned with a gabbro-pyroxenite axis. These are elements related to the ultramafic deposit [5].

The presence of Mg, to a lesser extent (positive), and of Ca, Na, and Ba, all negative (PC1 in **Figures 3(a)-(c)**) is at the origin of PC2 (20.333553%). Extraction of the elements Ca, Na, and Ba shows the presence of leaching likely due to hydrothermal fluids with the presence of carbonates. Vectors of these elements show an antithetical relationship with Al and LOI. A contribution of Mg for the formation of olivine and pyroxenes favors the development of Ni and Sc mineralization and (Ti, Fe, V) mineralization linked to magnetite rocks.

Whilst the presence of K, Si, Na, Ba (negative) to a lesser extent is linked to the PC3 factor (which represents 10.18587% of the variation) and is associated with felsic rocks and, the lower contribution of PC4 (7.146%) is associated with Si, Ka, Sr, Na and Ba, a negative series (**Figure 3(c)**). Principal components (PC1 to PC4) represent 84.1% of the overall variability and are the only ones for which the eigenvalues are far greater than 1.0 (**Figure 2**) [3] [12] [13]. The first two PCs represent 66.83% of the variability (46.5% and 20.33%, respectively) and illustrate a covariance of varying degrees between the group of variables. These spatially separated sequences of elements PC1-PC2-PC3-PC4 are directly apparent (**Table 1**).

Table 1. PCs summary and interpretations.

PC	Eigenvalue	Variance explained %	Cumulative variance explained %	Associations	Interpretations
PC1	9.30%	46.50%	46.5	Fe, Ni, Co, Cr, Mn, V, Si, K	Magmatic signature of Fe-Ti rich ultramafic Its inverse relationship with felsic component
PC2	4.07%	20.30%	66.83	Mg, Ca, Na, Sr	Secondary alteration processes, hydration (LOI)
PC3	2.04%	10.20%	77.01	Al, Ti, V, Ni, Zn, Sr	Crustal contamination events incorporation of Aluminous phases or titaniferous minerals
PC4	1.43%	7.10%	84.54	P, Ba, K, Ti, Cr	Phosphate-serpentinization

In **Figure 3(a)**, PC1-PC2 biplot diagram where PC1 (Axe X) represents primary magmatic processes versus secondary process on the positive side (right), Si indicates silica enrichment due to late magmatic stages or alteration. LOI suggests

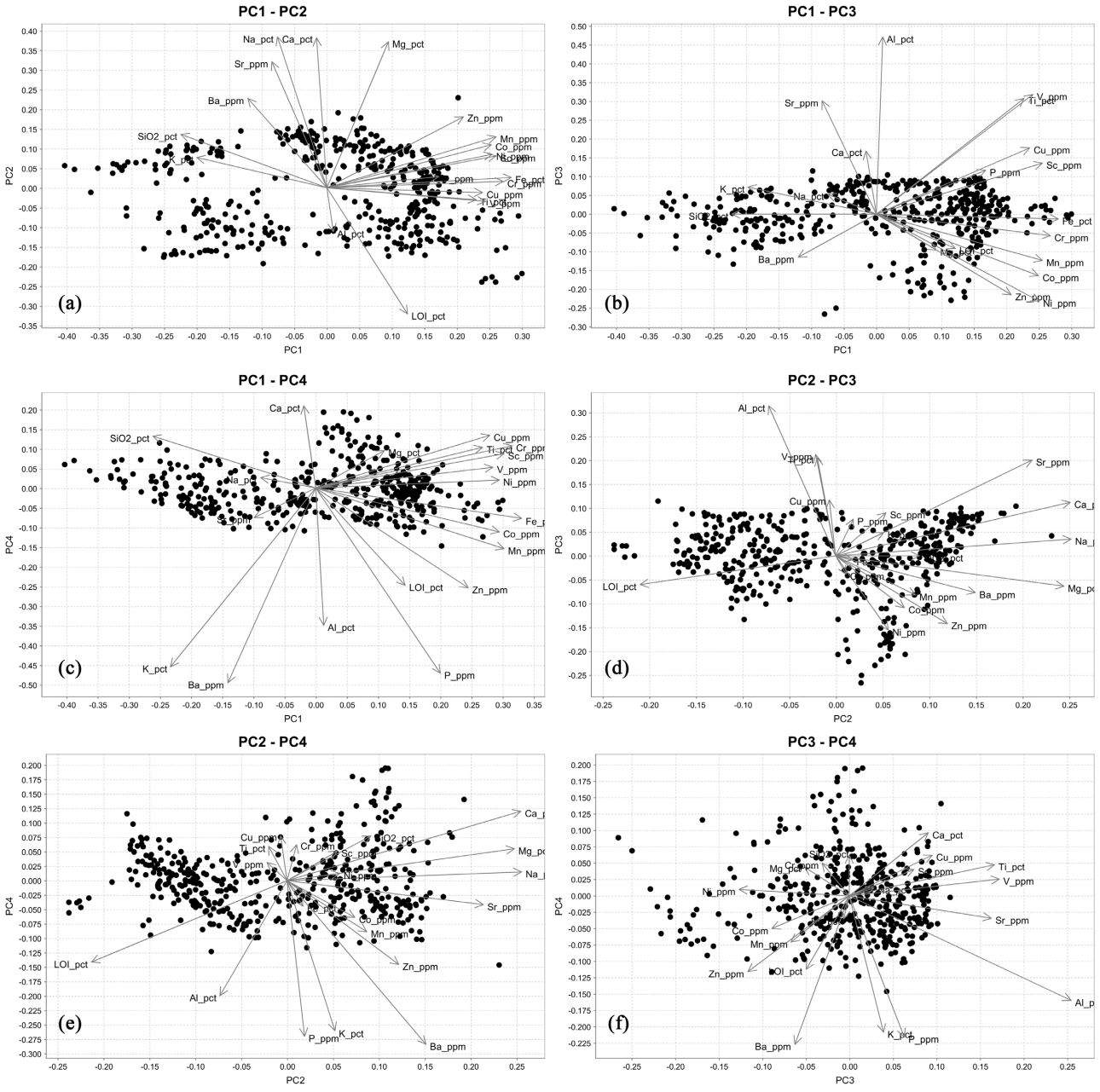

Figure 3. (a) showing primary magmatic process vs, secondary and traces elements enrichment; (b) Primary magmatic process with sulfide mineralization; (c) Contrast between magmatic and hydrothermal process; (d) Magmatic signature showing olivine, pyroxene and chromite with alteration fluid and different phases of crystallization; (e) magmatic suit with elements such as Cr, Ni, Mg, Ti with olivine, chromite, titanium magnetite. A sulfide mineralization potential zone and Ni remobilization process; (f) Late magmatic evolution, show magmatic fractionation processes and overprinting hydrothermal alteration.

secondary hydration (serpentinization), or carbonation and Ba may reflect hydrothermal fluids, indicating post-magmatic alteration. The negative side (Left) on the same **Figure 3(a)**; Na, Ca, and Mg represent primary ultramafic mineralogy (e.g., olivine, pyroxenes) and Ti associated with ilmenite/magnetite indicating primary Fe-Ti oxides. PC2 (Axe Y), traces elements enrichment, the positive side (Top) shows Mn, Co, Cu, Zn bound to sulfide phases or late fluids, suggesting

hydrothermal overprinting or sulfide mineralization. Whereas the negative side (Bottom) shows no significant variables, probably reflecting background noise. Thus, this first bivariate shows (1) a primary magmatic signature (PC1 Negative), dominated by Mg, Ca, Ti, reflecting ultramafic host rocks (olivine, pyroxenes) and Fe-Ti oxides. The low Si content corresponds to typical ultramafic compositions. (2) an alteration/secondary process (PC1 Positive), highlighted by SiO_2 and LOI, indicating serpentinization or silicification, with Ba suggesting fluid input and, (3) Traces element enrichment (PC2 Positive), high Mn, Co, Cu, Zn contents could indicate sulfide mineralization (e.g. chalcopyrite, pentlandite) or late hydrothermal remobilization.

PC1-PC3 biplot at PC1 (X-axis), the dominant source of variance, probably reflects primary magmatic processes as opposed to fluid-related processes (see **Figure 3(b)**). Here is a positive PC1 (Right), a variable including Sr, Ca, Na and Ba. These could suggest plagioclase fractionation, carbonate alteration, or the influence of hydrothermal fluids (e.g., alkali-rich fluids or carbonatitic metasomatism). A negative PC1 (Left), variables including Al, Cr, Sc, P and REE (rare earths?). These elements reflect mafic-ultramafic minerals (e.g., spinel, pyroxene) and could indicate primary Fe-Ti-Cr magmatic assemblages or apatite enrichment. PC3 (Y Axis) captures secondary variability, potentially related to redox or trace metal signatures, showing positive PC3 (Top), a variable including Cu, Zn and Zr. Cu-Zn suggests sulfide mineralization (e.g., chalcopyrite, sphalerite), while Zr could indicate serpentinization process or mantal source (e.g., zircon) and negative PC3 (bottom) with variables including Cr and Sc (positive), associated with chromite and pyroxenes, representing residual magmatic minerals in unweathered ultramafic. In conclusion, negative PC1 values correspond to zones of main mineralization (e.g., magnetite-ilmenite-chromite), Fe-Ti-Cr mineralization. Positive PC1 values highlight fluid-affected zones, with possible remobilization of metals, a Fluid-altered zone. High Cu and Zn contents (positive PC3) could indicate Ni-Cu-EGP prospects, hence sulfide potential. High P contents could suggest the presence of apatite associated with rare earths. High Sr and Ba levels indicate fluid flow conduits, while low Al a possible leaching (e.g., serpentinization), reflecting a zone of alteration.

On PC1-PC4 biplot diagram (**Figure 3(c)**), the PC1 factor (X axis), a main source of variance, contrasting magmatic (negative) and hydrothermal (positive) processes, range from −0.50 to 0.35. Positive PC1 (Right) shows SiO_2, LOI, Al, K, Ba, P, Zn, fluid-dominated zones (silicic alteration, hydration, hydrothermal fluids) while negative PC1 (Left) with Ca, Ti, Cr, V, Ni, Fe, Co, Mn primary magmatic minerals (clinopyroxene, chromite, magnetite). As for PC4 (Y axis), minor but distinct variability, potentially linked to redox conditions or late weathering, ranges from 0.40 to 0.20. Positive PC4 (Top), Cu, Zn, Ba, sulfide enrichment, or oxidizing fluids (chalcopyrite, barite), while negative PC4 (Bottom), Cr, Ni, Co, reducing conditions (chromite, pentlandite). This diagram shows the potential for polymetallic mineralized zones as follows PC1 Negative + PC4 Negative, main Fe-

Ti-V-Cr-Ni mineralization (magnetite, ilmenite, chromite) and PC1 Positive + PC4 Positive, hydrothermal intersections (sulfides, barite, phosphates). The presence of alteration and sulphides zones is marked by high SiO_2 + LOI values, potential zones for metal remobilization (serpentinization), and high Ba + P values, indicative of sulphides or rare-earth targets, while the potential for sulphides mineralization is marked by high Cu-Zn-Ba values (PC4 positive), indicative of potential for Cu-Ni-EGP mineralization.

For PC2-PC3 biplot diagram (**Figure 3(d)**), PC2 (X axis) where negative PC2 shows a magmatic signature (e.g., olivine, pyroxene, chromite) and positive PC2 indicates fluid alteration (e.g., serpentinization, carbonation). PC3 (Y axis) or negative PC3 shows elements and arrangements emanating from early crystallization products and, positive PC3 reflects late fractionation and alteration. Here the key variable groups are, (1) Primary magmatic package (PC2-Negative, PC3-Negative) shows variables such as Mg, Cr, Ni, Co with minerals such as olivine, chromite, pyroxenes, indication for cumulative zones of high mineralized potential. (2) Fluid alteration signatures (PC2-Positive) with variables such as LOI, Ba, Sr, indicating a fluid alteration signature and therefore the potential for remobilized Ni-Cu sulfides. And finally (3) Late enrichments (PC3-Positive) with elements such as Cu, Zn, P, showing potential for hydrothermal sulfide lenses or PGE. Ba/Sr peaks mark alteration fluid conduits, while a high LOI + SiO_2 indicates serpentinized shear zones.

PC2-PC4 biplot diagram, here the PC2 (X Axis), where PC2-negative side has a primary signature of ultramafic rocks, dominated by chromium (Cr), nickel (Ni), and magnesium (Mg) (**Figure 3(e)**). These elements are typical of primary magmatic phases, whereas PC2 on the positive side shows elements mobile in fluids, such as barium (Ba), potassium (K), phosphorus (P), and zinc (Zn). These elements indicate hydrothermal or metasomatic processes. PC4 (Y Axis), shows PC4 negative side, early magmatic phases, marked by titanium (Ti), magnesium (Mg), and chromium (Cr). PC4-positive side of late processes, including copper (Cu), scandium (Sc), and oxygen (O_2). These elements are associated with sulfide segregation and oxide-sulfide boundaries. The analysis identified several mineralization clusters, each revealing distinct geological processes, a magmatic suite (PC2-, PC4-) has elements such as Cr, Ni, Mg, Ti, and minerals such as chromite, olivine, titaniferous magnetite. This cluster reflects primary magmatic processes and suggests a high potential for Cr-Ni-Ti mineralization. A potential sulfide mineralization (PC4+) has elements such as Cu, Sc, O_2, or Cu-Sc coupling indicates magmatic sulfide segregation. The presence of O_2 serves as an indicator for the boundary between oxidized and sulfidized phases. Fluid alteration (PC2+) is marked by elements such as Ba, K, P, Zn reflecting a carbonation process and alkaline metasomatism. These elements mark zones of nickel remobilization and hydrothermal fluid pathways. Ba/K peaks can identify fluid conduits, while phosphorus (P) can indicate potential for rare earths associated with apatite.

The PC3-PC4 biplot (**Figure 3(f)**) provides essential information on late mag-

matic evolution, hydrothermal overprinting, and metasomatic alteration. PC3 (X axis), magmatic fractionation and alteration processes, distinguishes between early and late magmatic processes. Negative PC3 values correspond to early magmatic crystallization, indicated by variables such as Ti and V, suggesting primary oxidized minerals such as titanomagnetite and vanadiferous spinels. Positive PC3 values, on the other hand, reflect late fractionation or alteration, often associated with sulfide mineralization (Cu, Zn). PC4 (Y axis), the PC4 axis highlights redox conditions and fluid interactions. Negative PC4 values correspond to reduced mineral assemblages, typical of primary magmatic conditions. Positive PC4 values indicate oxidized or fluid-rich zones, marked by elements such as Ba, Sr, and LOI, suggesting carbonate-chlorite alteration and possible nickel remobilization. Primary magmatic signatures (PC3-Negative, PC4-Negative) represent zones of primary oxidized mineralization, characterized by high Ti and V concentrations.

Sulfide potential (PC3-Positive, PC4-), magmatic sulfides (PC3+, PC4-) may appear as primary sulfide lenses, while hydrothermal overprinting (PC3+, PC4+) suggests Cu-Zn enrichment due to fluid interactions. Alteration fluids (PC4-Positive) with high Ba and Sr levels highlight fluid infiltration paths, crucial for identifying metasomatic fronts and possible Ni remobilization. The gradient between Ti-V (PC3-) and Cu-Zn (PC3+) reveals a fractionation sequence, while PC4 variations define redox boundaries.

4.3. Cluster Analysis

K-Means Clustering

Cluster analysis (**Figures 4-6**) is a statistical technique that groups object in a population based on their similar characteristics to create clusters (groups) of individuals [7] [12] [14]. This type of method first creates pairs or groups, by clustering two objects or more with the most similar values of variables on the one hand. On the other, it has data for each chemical element evaluated in each participant. Though in K-means the elements are organized into groups of two or more, based on their proximity as indicated by their mean values or, could contain a single element (outliers) [3] [12].

In this study the clustering analysis used is K-means, which aims to group samples to minimize variation within groups and maximize variation between groups; this method has been successfully applied to lithogeochemical data individuals [7] [12] [14]. It is then possible to calculate the various statistical parameters for each group, including the average chemical composition of each. Determining the average chemical composition of the cluster enables a theoretical petrological name to be assigned to the cluster (lithogeochemical determination) and compared with the petrographic determination in the field supported by [5] & [15] in their respective studies.

But there is a limitation in using K-means clusters as it tends to form groups of similar size (in Euclidean space), whereas this can cause problems for raw, untransformed data, where variables often differ by several orders of magnitude in

terms of absolute abundance, meaning it works best for spherically distributed data [16]. Principal components are best suited to the K-means cluster, as they are both centered and scaled [12] [13]; and use the Kaiser-Guttmann rule which states that the eigenvalue must be greater than 1.0 (**Figure 2**) for conventionally scaled data for the number of principal components selected for inclusion in K-means clustering [13].

1) K-means = 6

An analysis of the results (**Figures 6(a)-(f)**) by clustering shows, a) a PC1 representing a major geochemical gradient, probably reflecting the compositional continuity (Junction) between ultramafic and mafic. Strong contributions from Mg, Ca and Sr suggest that this PC captures mafic-ultramafic mineralogy. b) PC2 shows strong associations with Al, P, K and Ba, potentially representing secondary alteration processes or felsic contamination components. c) PC3 correlates with transition metals (Ni, Co, Mn, Zn) and SiO_2, possibly reflecting sulfide mineralization or serpentinization processes. d) PC4 is associated with trace elements such as Ti, Sc, V, and some transition metals, possibly representing accessory mineral phases [12].

An association of notable elements indicating a mafic-ultramafic signature with elements such as Mg, Ca, Sr, Na clustering in the PC1-PC2 space. Alteration indicators Al, K, Ba, LOI (loss on ignition) show similar behavior. Sulfide-related elements Ni, Co, Zn, Mn often cluster together, and the SiO_2 component appears as a distinct vector in several graphs. The K-means clustering plot shows the sum of squares (variance) as a function of the number of clusters (K). Key Observations are, a) The "**elbow**" method suggests an optimal K where the variance reduction begins to flatten (**Figure 4**). The graph shows a reduction in variance up to at least K = 6, (but the exact optimal K is unclear here. b) For an ultramafic deposit, one would expect natural clusters corresponding to different ultramafic lithologies (dunite, harzburgites, lherzolite), alteration zones (serpentinized vs. fresh) and mineralized zones (sulfide-bearing vs. sterile). c) The high initial variance (approx. 2500) suggests considerable geochemical heterogeneity in the dataset [3].

A geological interpretation for the NGU ultramafic deposit shows a) The PC1 gradient probably represents the primary magmatic differentiation trend, from the most depleted (Mg-rich) to the least depleted compositions. b) PC2 may represent secondary processes such as serpentinization (contributing Al, K, Ba) or other fluid-related alteration. c) Transition metal associations (Ni, Co, etc.) in PC3 and PC4 could indicate sulfide mineralization, common in ultramafic systems, while d) SiO_2 behavior (SiO_2 mobility) suggests that it does not simply follow the primary magmatic trend, but could reflect secondary silicification [5].

In this study with an average K = 6 it is clear that further study is essential and, a) determine the optimum K so a clearer plot of intra-cluster variance as a function of K would help identify the true "elbow" point for cluster number selection. b) Validate clusters geologically by comparing statistical clusters with geological mapping to ensure they have petrological significance. c) Examine element ratios

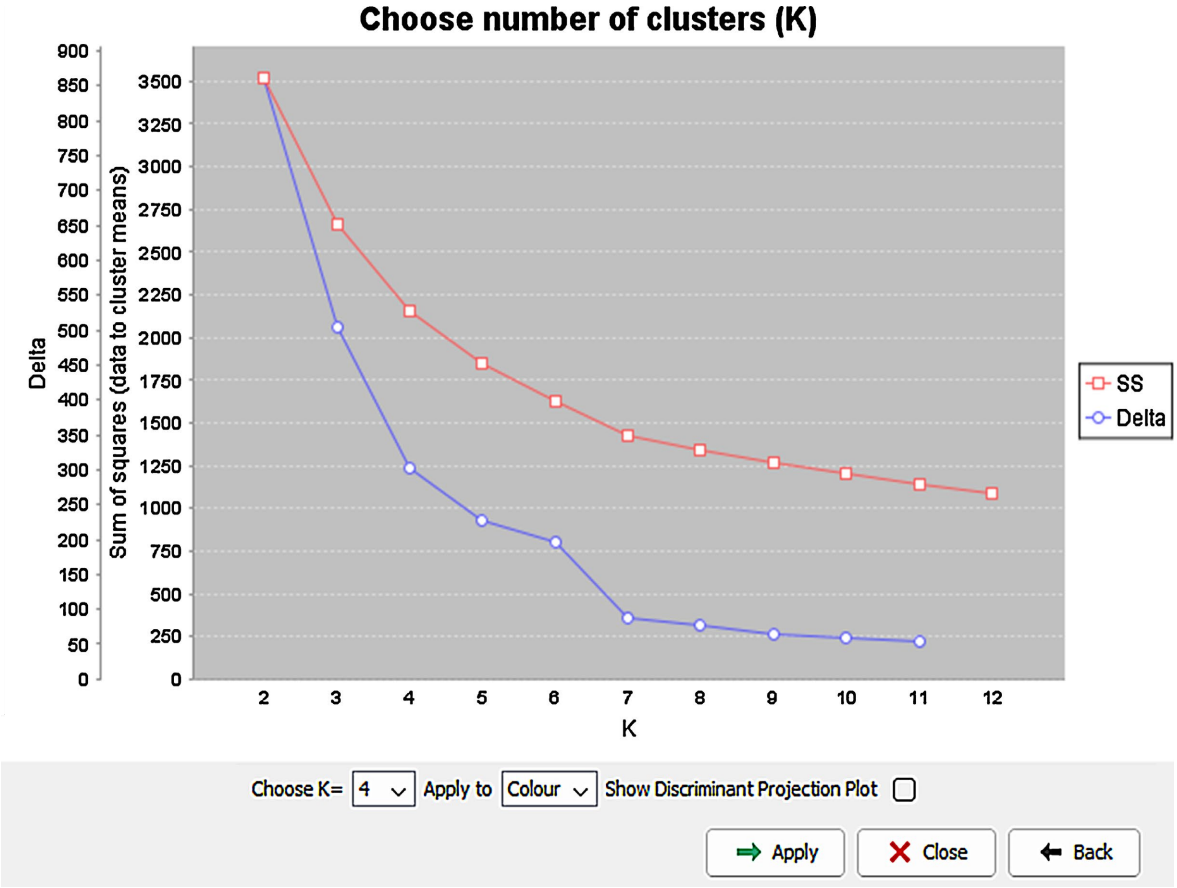

Figure 4. Graphic showing high initial variance and optimal K. The K-means clustering plot shows the sum of squares (variance) as a function of the number of clusters (K).

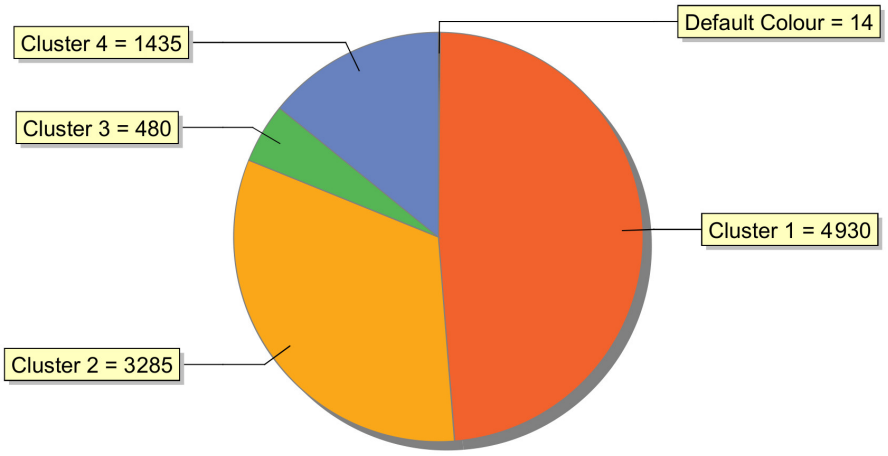

Figure 5. Pie chart showing clustering K = 4. Red: unweathered ultramafic lithology (Mg-Fe-rich, low SiO_2). Orange colored: Fe-Ti mineralized zones (enriched in Ti, Fe, Cr, V). Green: hydrothermal altered domains (carbonate/serpentine-rich?). Blue: transitional or mixed lithologies (e.g., silicified ultramafic).

(for ultramafic systems), such as Mg/Si, Mg/(Fe + Mg) or Ni/MgO could provide clearer clustering. d) Perform spatial analysis by mapping cluster assignments to see if they correspond to spatial patterns in the deposit [12].

Figure 6. Biplots clustering showing samples color-coded using K-means clustering: K = 6 (a)-(f) and K = 4 (a, b, c, d, reference to pie chart presentation).

2) K-means = 4

In this analysis, PC1 (major lithological control) reflects the primary composition of ultramafic rocks (Mg, Ca, Na), typical of magmatic cumulates such as dunites. Its negative correlation with Al and K underlines its opposition to weathering processes. PC2 captures the effects of serpentinization and metasomatic fluids (Al, K, Ba), revealing rock-fluid interactions, while PC3 and PC4 isolate key elements such as Ni, Co, and Ti, associated with sulfides and accessory minerals, respectively. The presence of SiO_2 in PC3 suggests zones of silicification, potentially linked to hydrothermal circulation. The correlation between Ni and Co in PC3

could indicate remobilized sulfide mineralization [17]. Optimal cluster validation shows significant variance reduction up to K = 4 with diminishing returns beyond 4 clusters, justifying the selection and/or the four (4) clusters solution illustrated on the curve and supported by the pie chart (**Figure 5**). The clustering results and the choice of K = 4 clusters are justified by optimal variance reduction. Each cluster corresponds to a distinct geological facies (**Figures 6(a)-(d)**):

a) Cluster 1 (4930 samples), unweathered ultramafic lithology (Mg-Fe-rich, low SiO_2).

b) Cluster 2 (3285 samples), Fe-Ti mineralized zones (enriched in Ti, Fe, Cr, V).

c) Cluster 3 (480 samples), hydrothermal altered domains (carbonate/serpentine-rich?).

d) Cluster 4 (1435 samples), transitional or mixed lithologies (e.g., silicified ultramafic).

- Outlier values (14 samples), exotic lithologies (e.g., pegmatitic veins).

Cluster 1 involves fresh, unaltered rocks; Clusters 2 and 4 are priority targets for Fe-Ti ore and associated alteration halos, while Cluster 3 represents alteration gradients (talc-carbonate serpentinization) [5]. Though optimal clustering (K = 4) grouped samples into fresh ultramafic Rocks with high Mg-Fe, low SiO_2, a Fe-Ti mineralized zones (3285 samples) enriched in Ti, Fe, Cr, V and hydrothermally altered domains (480 samples) with carbonate and serpentine-rich and, lastly a transitional lithologies (1435 samples) with mixed compositions. The K = 4 choice is consistent with geological facies grouped from samples but also aligned with the PCA geological process finding (**Table 1**) and, PC1 to PC4 explaining 84.14% of total variance observed. PC1 to PC4 eigenvalues are > 1 [13], whereas the remaining PCs (PC5, PC6…) are below (<) 5% each, hence does not match [18] position, suggesting retaining components presenting > 5% variance each for geological explanation.

5. Discussion and Implication for Exploration

Ultramafic Fe-Ti deposits are complex geological phenomena resulting from magmatic and hydrothermal processes [2]. To identify their mineralogical associations, petrological implications, and reconstruct their genesis at NGU, PCA is used to identify the processes (magmatism, alteration), while K-means localizes them spatially. The results show that the first three (3) principal components (PC1, PC2, PC3) together explain 77.01% of the total variance. This result is consistent with the observations of [18], who recommends retaining components explaining at least 70% - 80% of the variance. The scree plot shows a sharp decrease after PC3, which explains this choice, according to the Kaiser criterion [13], which suggests retaining eigenvalues > 1. However, according to [19], retaining components according to the Kaiser criterion alone could lead to an underestimation of the number of significant principal components. A parallel analysis [20] might be necessary to complement this approach to confirm this selection.

Magmatic differentiation and their alteration are supported by an opposition between elements related to primary minerals (Mg, Ca) to those influenced by alteration (SiO_2) but also by loss on ignition (LOI). This distinction probably suggests magmatic differentiation processes in the stratified intrusions [21]. While [1] described the NGU deposit to be constituted of a dunite (olivine rock) core, a concentric pattern zoned intrusive body followed by wehrlite envelop then olivine-pyroxenite which is surrounded by pyroxenite rim.

There is a strong opposition (PC1) between mafic elements (Fe, Cr, Ni) and silica (SiO_2) which reflects a fundamental process of magmatic differentiation (Mafic-felsic dichotomy); opposition was explained by [22] in his reaction series.. In this area the Na-Sr association, characteristic of plagioclases and Ba of hydrothermal fluids, showing a hydrothermal overprint that are generally observed or similar to carbonatite systems [23]. The dominance of Ca, Na and Mg in PC2 can be interpreted as an introduction of carbonate and, or a plagioclase signature, consistent with the observations of [24] on continuous feldspar series. The strong Ca-Sc correlation (0.68) particularly supports the plagioclase signature, as scandium is typically incorporated in calcic pyroxenes [25], although no plagioclase presence was demonstrated in the NGU deposit on petrographic study [1] or by virtual mineral calculations (CIPW) reporting high olivine and pyroxene and, presence of magnetite, ilmenite and apatite with no quartz or feldspar.

NGU presents a signature of Fe-Ti oxides forming titaniferous magnetite and chromite spinels which is supported by the correlation between Fe, Ti, and Cr, it is characteristic of ultramafic deposits [26]. While Cu and Zn suggest a late mobilization of sulfides, suggesting magmatic fractionation processes [17]. On the other hand, the negative association between SiO_2 and Fe is particularly remarkable, with a coefficient of −0.88. This strong anticorrelation is explained by the incompatibility of these elements during fractional crystallization, as demonstrated by [27] in their petrogenetic model. At the PC3 level (Sulfide Mineralization and Silica Mobility) the correlation between Ni, Co, Zn and SiO_2 is characteristic of ultramafic systems mineralized in sulfides [28]. However, [29] showed that in Komatiite-type deposits, SiO_2 is often associated with late remobilizations. A positive correlation with Ni could also indicate silicification associated with mineralizing fluids [30].

Ba-K and Mn-Co-Zn associations indicate potassium alteration followed by metal remobilization under hydrothermal conditions in metasomatic systems [31] but also in reducing environments [32]. The enrichment of Al, K and Ba in PC2 is characteristic of hydrothermal alteration processes, including serpentinization [33]. These elements are mobile in fluids and are much more present in water-rock reaction zones. The presence of Ba could also suggest crustal contamination, as documented in alkaline complexes [34]. The importance of Al and Sr in PC3 is consistent with the findings of [35] on alteration processes. However, the simultaneous presence of Sr also suggests an influence of alkali feldspars, as shown by [36] in their continental crust model.

According to [28] the minerals association in cluster 1 is typical of ultramafic-mafic layered complexes, which he describes in intrusions hosting Fe-Ti-V deposits. While [1], noted the absence of layer deposit in NGU marking its difference to Ural Alaskan type. The predominance of this cluster reflects fractional crystallization under stable magmatic conditions. Cluster 2 shows correlations with LOI (loss on ignition) and Ca, suggesting hydrothermal alteration transformation processes, such as serpentinization or carbonation, resulting from the interaction between ultramafic rocks and CO_2- or H_2O-rich fluids [37].

Localized concentrations of oxides representing Cluster 4, showing enrichment in Ti and Fe, which could correspond to zones of differential concentration of oxides, well observed in the "reef-type Fe-Ti" deposits of the Bushveld complex [38]. These accumulations often result from advanced fractional crystallization processes. While Cluster 3 represents accessory minerals such as sulfides (chalcopyrite, sphalerite, pyrite……), they are in the minority but show enrichments in Cu and Zn. These phases, often associated with late residual fluids present in differentiated magmatic systems [39].

Fundamentally a newly discovery Fe-Ti deposit [1] and, comparison from **Table 2** shows NGU representing a particular type of Fe-Ti ultramafic deposit

Table 2. Comparative analysis between NGueredonke, Lac Dore and Panzhihua.

Features	NGU—Guinea	Lac Dore—Canada	Panzhihua—China
Geodynamic setting	Syntectonic in Archean Craton shear zone	Synvolcanic Archean greenstone belt	Large igneous province, Continental rift setting
Host Rock	Dunite, Wehrlite and Pyroxenite	Anorthosite-Gabbro-leucogabbro	Gabbronorites, Pyroxenites
Plagioclase content	No plagioclase	Abundant	Moderate to Abundant
Major Oxide	Ultramafic with low Si, low Al, high MgO (25 - 35 wt%) and low SiO_2 (35 - 40 wt%) and low Al_2O_3 (0.5 - 2 wt%), the FeO_t (10 - 15 wt%) is high	Mafic with progressive high-Al, and moderate SiO_2 (45 - 50 wt%), very high Al_2O_3 (15 - 25 wt%) and FeO_t (10 - 20 wt%)	Ferrobasalt/Ferropicrites, moderate MgO (5 - 12 wt%), Moderate SiO_2 (45 - 50 wt%) and Al_2O_3 (10 - 15 wt%) with high FeO_t (15 - 25 wt%)
Ore Mineralogy	Disseminated-ilmenite (Ti-rich)-Cr bearing magnetite-No Chromite	Massive to semi massive layers/Bands-Magnetite-ilmenite-Apatite	Massive, Thick layers-titanomagnetite (+V)-ilmenite
Important trace elements	High Cr (>2000 ppm, High Ni, High Co, low incompatible elements (Zr, Y)-Ti/V variable	Low Cr, Ni, Co, high P_2O_5, Moderate incompatible elements	Moderate Cr, Ni, very high V, very low Ti/V ratio
Genetic Model	Polyphase ultramafic cumulate: Oxide saturation from successive injections of Ti-Fe rich, Al poor ultramafic magma in shear zone. And high fO_2 suppresses chromite	Fractional Crystallization of anorthositic magma: Fe-Ti oxides and apatite are formed by crystallization from highly evolved Fe-Ti-P-rich residual melts are separated from the anorthosite crystal mushes.	Liquid immiscibility and crystal settling, processes of fractional crystallization of ferrobasalt allow silicate liquid immiscibility and formation of Fe-Ti-P-rich oxide melts, which get mix together and form as massive layers.
References	Gloaguen *et al.* (2015) [1]	Charlier *et al.* (2010) [8]	Zhou *et al.* (2005) [40]

(zoned polyphase injection deposit) with high fO2 leading to Cr-bearing magnetite and disseminated ilmenite forming in unusual geodynamic setting (Archean Craton) instead of chromite formation in layers or pods [8] [38] [40].

Implication for Mineral Exploration

This study demonstrates that the deposit follows a model of at least two phases of magmatic fractionation with hydrothermal overprinting. The results of K-means and PCA analyses demonstrate:

1) The dominance of Fe-Ti oxides (Clusters 1 and 4, PC1-PC3), Ni-Cr in the high PC1 zones.

2) The presence of accessory sulfides (Cluster 3, PC1-PC3).

3) The influence of hydrothermal processes (PC2-PC4).

The Ba-Sr pair (PC2) could indicate fluid-enriched zones, similar to Kiruna-type deposits [41]. PC2 could guide the exploration of areas with metallotect potential (fluid corridors).

Priority targets could be Clusters 1 & 4, which are Fe-Ti rich zones, a priority for oxide exploration and exploitation. While cluster 3 may have potential in this huge shear zone (60 km long) for Cu-Zn sulfides, similar to Fe-Ti-P type deposits [38]. But Ni-Co rich clusters should be prioritized for sulfide analyses.

6. Conclusions

This study demonstrated the power of multivariate statistics in deciphering the complex geochemical signatures of ultramafic deposits. PCA and clustering effectively distinguished magmatic, alteration, and mineralization processes, providing a quantitative framework for exploration targeting. Key findings include 1) Magmatic Signatures dominated by Fe, Ni, Cr, and Mg, 2) Fluid Alteration highlighted by SiO_2, LOI, and Ba and 3) Mineralization Potential identified through Cu-Zn and Ni-Co associations. Integrating these methods with structural data could further refine exploration models, linking geochemical clusters to fault zones or other geological features.

The methods outlined in this study may be new to geologists, but they have been used in numerous other scientific disciplines for a considerable period and have given powerful results and are proficient in many disciplines. With the many different tools (Software) available, a minimal extra effort is needed, and some strong insights can be offered to mining or exploration by using multivariate techniques [3].

Acknowledgements

An early review of this draft by Dr. Chapiou and Pr. David Orodu, has significantly improved this paper. We especially thank Dr. Hamadou Ali for his comments and his interminable interest in our work from the beginning to its end; we are sincerely grateful.

Conflicts of Interest

The authors declare no conflicts of interest regarding the publication of this paper.

References

[1] Gloaguen, E., Augé, T., Bailly, L., Courrioux, G., Fullgraf, T. and Perin, J. (2015) A New Type of Large Ultramafic Intrusion-Hosted Fe-Ti-V Deposit in the West-African Archean Craton: The N'Guérédonké Complex, Guinea. 13*th SGA Biennial Meeting on Mineral Resources in a Sustainable World*, Nancy, August 2015, hal-04609019.

[2] Choubert, B. (1947) Géochimie des magmas et permanences statistiques. *Mémoires de la Société géologique de France*, **54**, 99 p.

[3] Gazley, M., Collins, K., Roberston, J., Hines, B., Fisher, L. and McFarlane, A. (2015) Application of Principal Component Analysis and Cluster Analysis to Mineral Exploration and Mine Geology. *AusIMM New Zealand Branch Annual Conference* 2015, Dunedin, 131-139.

[4] de Stabenrath, S. and Byrne, D. (2018) Geological Map of Guinea, Sems Exploration. http://www.sems-exploration.com

[5] Rollinson, H.R. (1993) Using Geochemical Data: Evaluation, Presentation, Interpretation. Longman Scientific and Technical, Wiley, New York, 352.

[6] Aitchison, J. (1982) The Statistical Analysis of Compositional Data. *Journal of the Royal Statistical Society Series B*: *Statistical Methodology*, **44**, 139-160. https://doi.org/10.1111/j.2517-6161.1982.tb01195.x

[7] Barker, S.L.L., Hood, S., Hughes, R.M. and Richards, S. (2019) The Lithogeochemical Signatures of Hydrothermal Alteration in the Waihi Epithermal District, New Zealand. *New Zealand Journal of Geology and Geophysics*, **62**, 513-530. https://doi.org/10.1080/00288306.2019.1651345

[8] Woodruff, L.G., Nicholson, S.W. and Fey, D.L. (2013) A Deposit Model for Magmatic Iron-Titanium-Oxide Deposits Related to Proterozoic Massif Anorthosite Plutonic Suite. Scientific Investigations Report.

[9] Aitchison, J. (1986) The Statistical Analysis of Compositional Data. Springer eBooks.

[10] Filzmoser, P., Hron, K., Reimann, C. and Garrett, R. (2009) Robust Factor Analysis for Compositional Data. *Computers & Geosciences*, **35**, 1854-1861. https://doi.org/10.1016/j.cageo.2008.12.005

[11] Reimann, C. and Filzmoser, P. (2000) Normal and Lognormal Data Distribution in Geochemistry: Death of a Myth. Consequences for the Statistical Treatment of Geochemical and Environmental Data. *Environmental Geology*, **39**, 1001-1014. https://doi.org/10.1007/s002549900081

[12] Jansson, N.F., Allen, R.L., Skogsmo, G. and Tavakoli, S. (2022) Principal Component Analysis and K-Means Clustering as Tools during Exploration for Zn Skarn Deposits and Industrial Carbonates, Sala Area, Sweden. *Journal of Geochemical Exploration*, **233**, Article ID: 106909. https://doi.org/10.1016/j.gexplo.2021.106909

[13] Kaiser, H.F. (1960) The Application of Electronic Computers to Factor Analysis. *Educational and Psychological Measurement*, **20**, 141-151. https://doi.org/10.1177/001316446002000116

[14] Hood, S.B., Cracknell, M.J. and Gazley, M.F. (2018) Linking Protolith Rocks to Altered Equivalents by Combining Unsupervised and Supervised Machine Learning. *Journal of Geochemical Exploration*, **186**, 270-280. https://doi.org/10.1016/j.gexplo.2018.01.002

[15] Gibson, S. (2003) Le Maitre, R. W. (ed.) 2002. Igneous Rocks. A Classification and Glossary of Terms. Recommendations of the International Union of Geological Sciences Subcommission on the Systematics of Igneous Rocks, 2nd Ed. xvi + 236 p. Cambridge, New York, Melbourne: Cambridge University Press. *Geological Magazine*, **140**, 367-367. https://doi.org/10.1017/s0016756803388028

[16] Templ, M., Filzmoser, P. and Reimann, C. (2008) Cluster Analysis Applied to Regional Geochemical Data: Problems and Possibilities. *Applied Geochemistry*, **23**, 2198-2213. https://doi.org/10.1016/j.apgeochem.2008.03.004

[17] Barnes, S. and Lightfoot, P.C. (2005) Formation of Magmatic Nickel Sulfide Deposits and Processes Affecting Their Copper and Platinum Group Element Contents. In: Hedenquist, J.W., Thompson, J.F.H., Goldfarb, R.J. and Richards, J.P., Eds., *One Hundredth Anniversary Volume*, Society of Economic Geologists, 179-213. https://doi.org/10.5382/av100.08

[18] Jolliffe, I. (2002) Principal Component Analysis. Springer Science & Business Media.

[19] Peres-Neto, P.R., Jackson, D.A. and Somers, K.M. (2005) How Many Principal Components? Stopping Rules for Determining the Number of Non-Trivial Axes Revisited. *Computational Statistics & Data Analysis*, **49**, 974-997. https://doi.org/10.1016/j.csda.2004.06.015

[20] Horn, J.L. (1965) A Rationale and Test for the Number of Factors in Factor Analysis. *Psychometrika*, **30**, 179-185. https://doi.org/10.1007/bf02289447

[21] Momme, P., Tegner, C., Kent Brooks, C. and Keays, R.R. (2006) Two Melting Regimes during Paleogene Flood Basalt Generation in East Greenland: Combined REE and PGE Modelling. *Contributions to Mineralogy and Petrology*, **151**, 631-632. https://doi.org/10.1007/s00410-006-0083-6

[22] Bowen, N.L. (1928) The Evolution of the Igneous Rocks. Princeton University Press.

[23] Doroshkevich, A.G., Prokopyev, I.R., Ponomarchuk, A., Savatenkov, V.M., Kravchenko, A.A., Ivanov, A.I., *et al.* (2020) Petrology and Geochemistry of the Late Mesozoic Dzheltula Alkaline Igneous Complex, Aldan-Stanovoy Shield, Russia: Constraints on Derivation from the Ancient Enriched Mantle Source. *International Journal of Earth Sciences*, **109**, 2407-2423. https://doi.org/10.1007/s00531-020-01909-6

[24] Deer, W.A., Howie, R.A. and Zussman, J. (2013) An Introduction to Rock-Forming Minerals. Mineralogical Society of Great Britain and Ireland eBooks.

[25] Le Bas, M.J. (1962) The Role of Aluminum in Igneous Clinopyroxenes with Relation to Their Parentage. *American Journal of Science*, **260**, 267-288. https://doi.org/10.2475/ajs.260.4.267

[26] Kamenetsky, V.S., Charlier, B., Zhitova, L., Sharygin, V., Davidson, P. and Feig, S. (2013) Magma Chamber-Scale Liquid Immiscibility in the Siberian Traps Represented by Melt Pools in Native Iron. *Geology*, **41**, 1091-1094. https://doi.org/10.1130/g34638.1

[27] Barnes, S.J., Cruden, A.R., Arndt, N. and Saumur, B.M. (2016) The Mineral System Approach Applied to Magmatic Ni-CU-Pge Sulphide Deposits. *Ore Geology Reviews*, **76**, 296-316. https://doi.org/10.1016/j.oregeorev.2015.06.012

[28] Cox, K.G., Bell, J.D. and Pankhurst, R.J. (1979) The Interpretation of Igneous Rocks. Springer. https://doi.org/10.1007/978-94-017-3373-1

[29] Naldrett, A.J. (2004) Magmatic Sulfide Deposits. Springer. https://doi.org/10.1007/978-3-662-08444-1

[30] Lesher, C.M. and Arndt, N.T. (1995) REE and Nd Isotope Geochemistry, Petrogenesis and Volcanic Evolution of Contaminated Komatiites at Kambalda, Western Aus-

tralia. *Lithos*, **34**, 127-157. https://doi.org/10.1016/0024-4937(95)90017-9

[31] Groves, D.I., Bierlein, F.P., Meinert, L.D. and Hitzman, M.W. (2010) Iron Oxide Copper-Gold (IOCG) Deposits through Earth History: Implications for Origin, Lithospheric Setting, and Distinction from Other Epigenetic Iron Oxide Deposits. *Economic Geology*, **105**, 641-654. https://doi.org/10.2113/gsecongeo.105.3.641

[32] Harlov, D.E., Meighan, C.J., Kerr, I.D. and Samson, I.M. (2016) Mineralogy, Chemistry, and Fluid-Aided Evolution of the Pea Ridge Fe Oxide-(y + REE) Deposit, Southeast Missouri, Usa. *Economic Geology*, **111**, 1963-1984. https://doi.org/10.2113/econgeo.111.8.1963

[33] Mavrogenes, J., Frost, R. and Sparks, H.A. (2013) Experimental Evidence of Sulfide Melt Evolution via Immiscibility and Fractional Crystallization. *The Canadian Mineralogist*, **51**, 841-850. https://doi.org/10.3749/canmin.51.6.841

[34] Evans, B.W. (2010) Lizardite versus Antigorite Serpentinite: Magnetite, Hydrogen, and Life(?). *Geology*, **38**, 879-882. https://doi.org/10.1130/g31158.1

[35] Pearce, J.A. (2008) Geochemical Fingerprinting of Oceanic Basalts with Applications to Ophiolite Classification and the Search for Archean Oceanic Crust. *Lithos*, **100**, 14-48. https://doi.org/10.1016/j.lithos.2007.06.016

[36] Nesbitt, H.W. and Young, G.M. (1982) Early Proterozoic Climates and Plate Motions Inferred from Major Element Chemistry of Lutites. *Nature*, **299**, 715-717. https://doi.org/10.1038/299715a0

[37] Taylor, S.R. and McLennan, S.M. (1985) The Continental Crust: Its Composition and Evolution: An Examination of the Geochemical Record Preserved in Sedimentary Rocks. Blackwell Science, Oxford, 312.

[38] Charlier, B., Namur, O., Bolle, O., Latypov, R. and Duchesne, J. (2015) Fe-Ti-V-P Ore Deposits Associated with Proterozoic Massif-Type Anorthosites and Related Rocks. *Earth-Science Reviews*, **141**, 56-81. https://doi.org/10.1016/j.earscirev.2014.11.005

[39] Mungall, J.E. and Naldrett, A.J. (2008) Ore Deposits of the Platinum-Group Elements. *Elements*, **4**, 253-258. https://doi.org/10.2113/gselements.4.4.253

[40] Zhou, M., Robinson, P.T., Lesher, C.M., Keays, R.R., Zhang, C. and Malpas, J. (2005) Geochemistry, Petrogenesis and Metallogenesis of the Panzhihua Gabbroic Layered Intrusion and Associated Fe-Ti-V Oxide Deposits, Sichuan Province, SW China. *Journal of Petrology*, **46**, 2253-2280. https://doi.org/10.1093/petrology/egi054

[41] Smith, M.P., Gleeson, S.A. and Yardley, B.W.D. (2013) Hydrothermal Fluid Evolution and Metal Transport in the Kiruna District, Sweden: Contrasting Metal Behaviour in Aqueous and Aqueous-Carbonic Brines. *Geochimica et Cosmochimica Acta*, **102**, 89-112. https://doi.org/10.1016/j.gca.2012.10.015